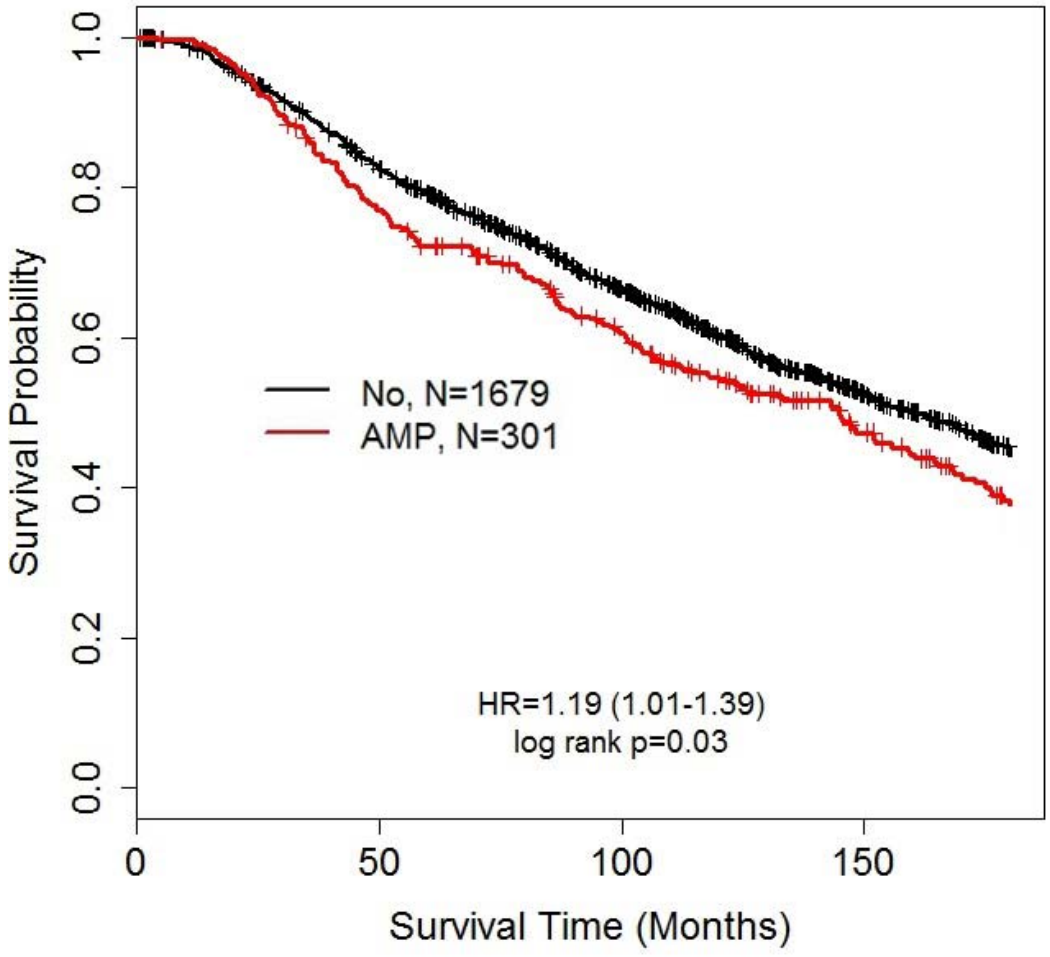


**Supplemental Figure 1. *ADHFE1* amplification (AMP) in breast tumors is associated with decreased survival.** HR: hazard ratio with 95% confidence interval. METABRIC dataset.

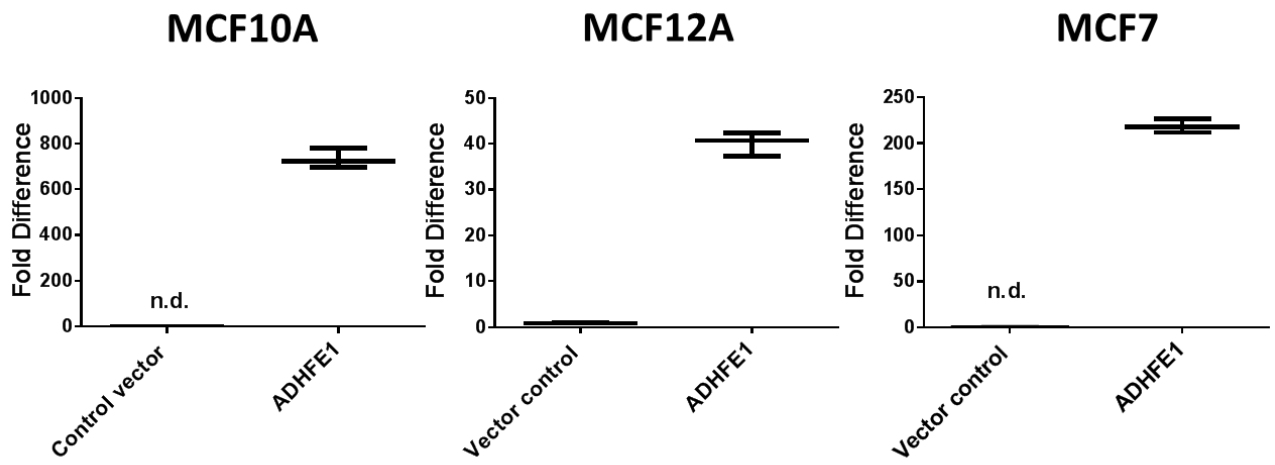


**Supplemental Figure 2. Up-regulation of *ADHFE1* in MCF10A, MCF12A, and MCF7 cells after lentiviral infection with the *ADHFE1* expression vector.** Shown are qRT-PCR measurements of relative expression in cells transduced with the *ADHFE1* expression vector (ADHFE1) or a control vector. *ADHFE1* expression levels were normalized to 18s rRNA expression. Endogenous expression of *ADHFE1* in the vector control cells was either very low or undetectable (n.d.). Therefore, fold differences are estimates only. Cells were selected with puromycin for stable transgene expression.

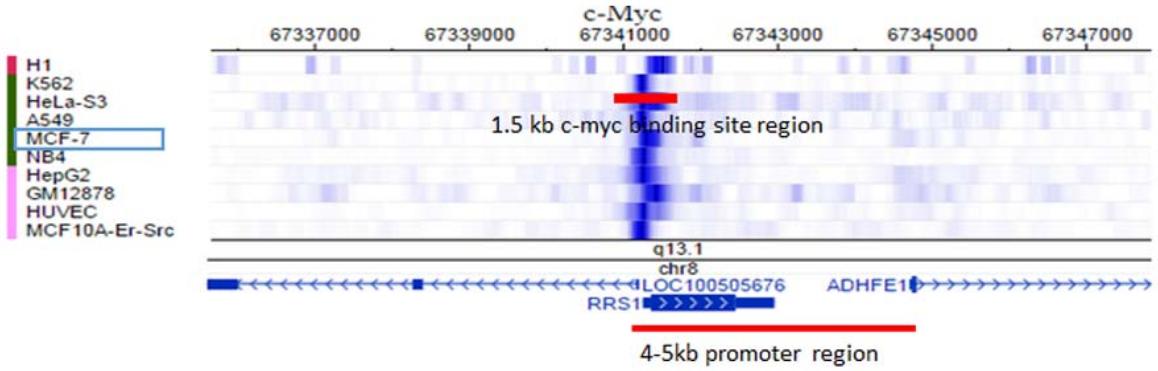


**Supplemental Figure 3. A Myc binding site is located near the promoter region of human *ADHFE1*.** Shown are ENCODE chip-seq data for a MYC binding site near the *ADHFE1* locus. However, this binding site is upstream of the *ADHFE1* promoter and located within the *RRS1* locus, making *RRS1* the more likely target gene of MYC.

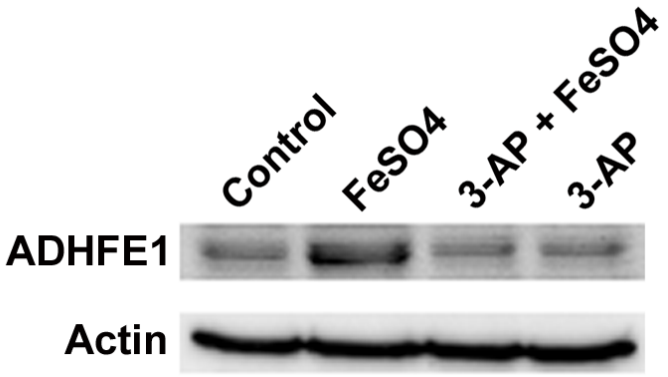


**Supplemental Figure 4. Western blot showing ADHFE1 protein expression.** Treatment of human mammary epithelial cells (HMEC) with the $Fe^{2+}$ chelator, 3-Aminopyridine-2-carboxaldehyde thiosemicarbazone (3-AP), inhibits $FeSO_4$-induced up-regulation of ADHFE1. HMEC were pre-treated with 0.5 µM 3-AP and then exposed to 0.5 mM $FeSO_4$ in the medium.

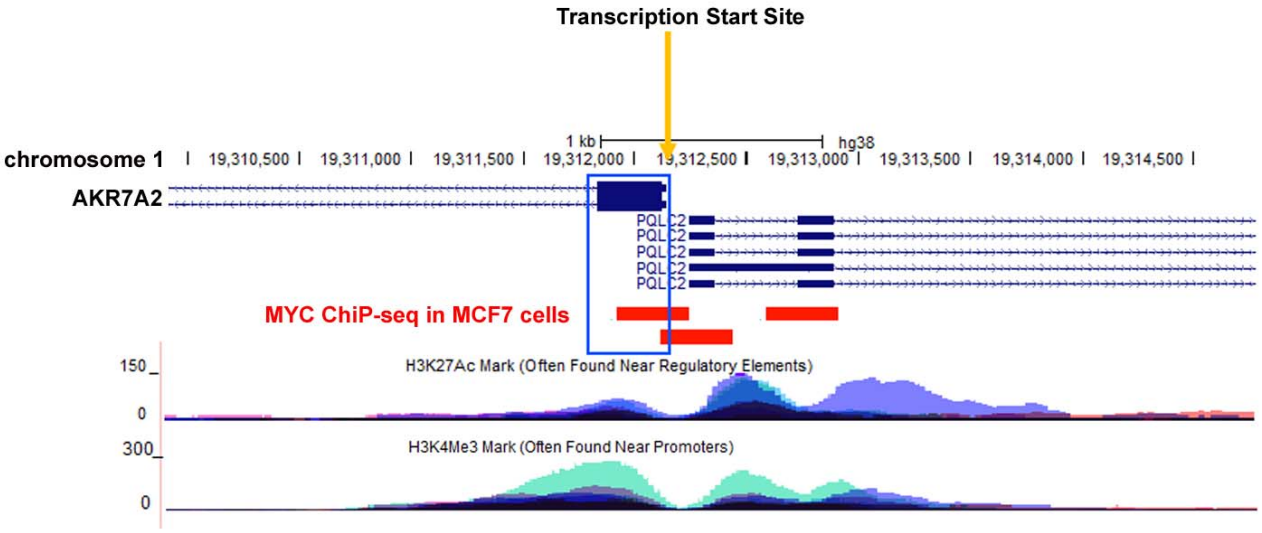


**Supplemental Figure 5. Myc binding sites in the promoter region of human *AKR7A2* in MCF7 cells.** Shown are ENCODE chip-seq data for MYC binding within the *AKR7A2* promoter region. Blue box shows the transcription start site for *AKR7A2* and the overlap with chip-seq-validated Myc binding sites (red boxes). This region overlaps with a region of increased histone 3 lysine acetylation and trimethylation, which also indicates transcriptional activation in this region.

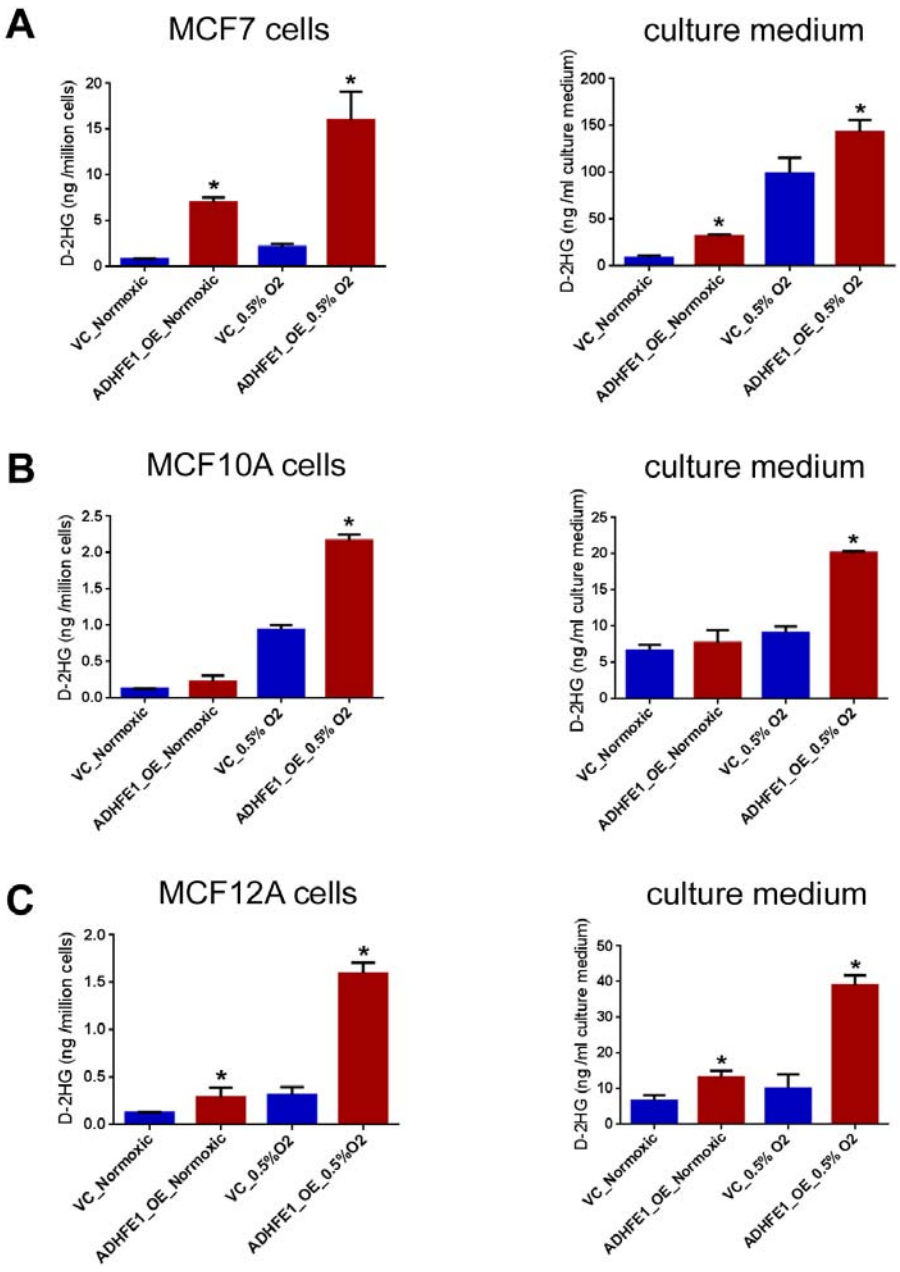


**Supplemental Figure 6. Intracellular and secreted D-2-hydroxyglutarate (D-2HG) under normoxic and hypoxic conditions (0.5% $O_2$) in *ADHFE1*-overexpressing cells.** Shown is abundance of D-2HG in cell extracts and culture medium of *ADHFE1*-overexpressing (ADHFE1-OE) versus vector control (VC) cells (n = 3 each, mean ± S.D.) for MCF7 (**A**), MCF10A (**B**), and MCF12A (**C**) cells. **P* < 0.05, versus vector control (two-sided t-test). Normoxic cells were cultured under standard conditions (21% oxygen) while hypoxic cells were cultured with 0.5% oxygen for 24 hrs (see methods).

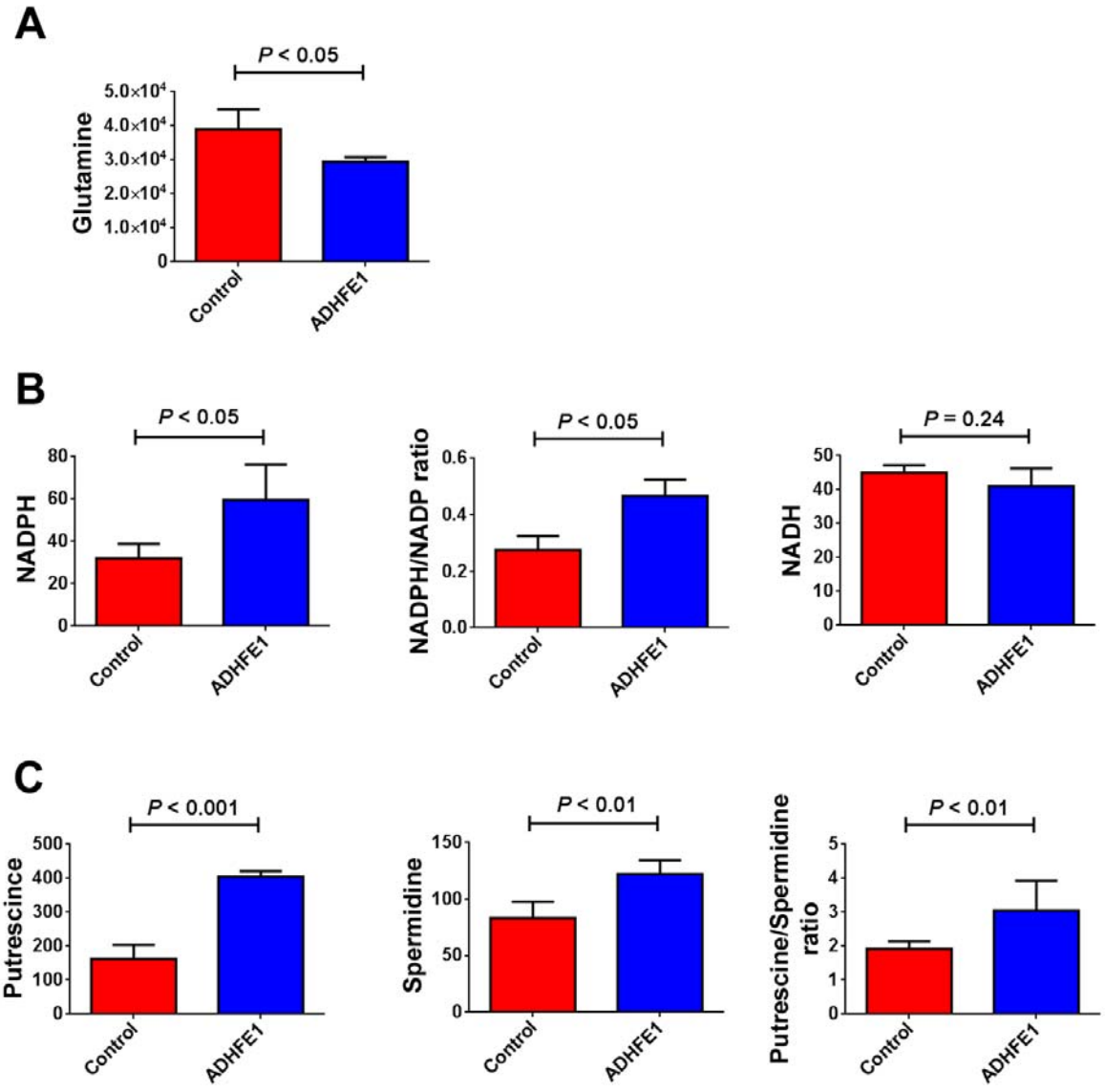


**Supplemental Figure 7. ADHFE1-induced metabolic alterations in MCF12A human mammary epithelial cells.** Shown are differences in metabolite abundance between *ADHFE1*-overexpressing MCF12A cells versus control cells. Reduced glutamine (**A**), increased NADPH (but not NADH) (**B**), and increased polyamines levels (**C**) in MCF12A cells with up-regulated ADHFE1. Metabolite concentrations are reported as pmol/$10^6$ cells (n = 4 each, mean ± S.D.). Two-sided t-test for statistical significance testing.

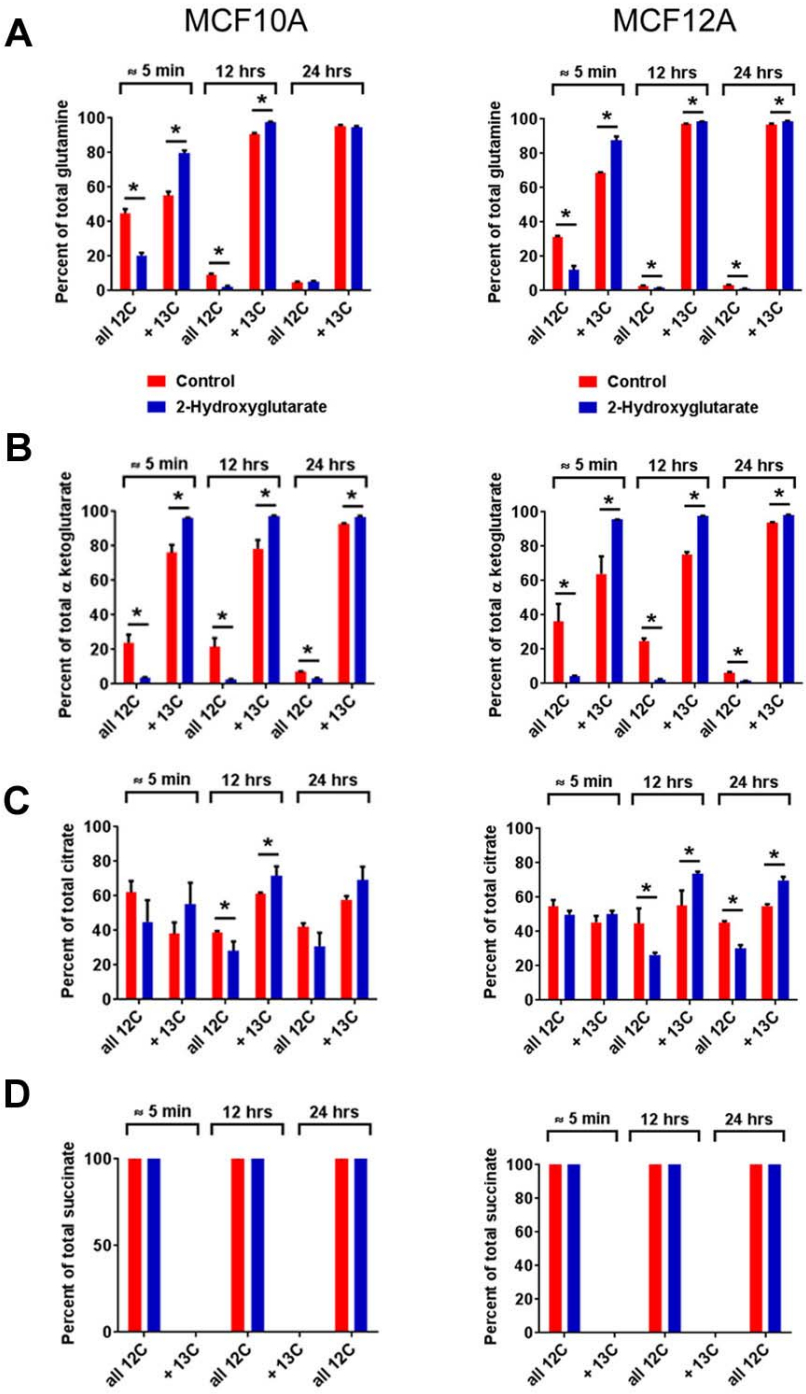


**Supplemental Figure 8. Increased incorporation of glutamine-derived 1-$^{13}$C label into α-ketoglutarate and citrate in cells treated with cell-permeable D-2HG.** MCF10A and MCF12A cells were cultured with cell permeable D-2HG (1 mM octyl-2HG) in presence of 1-$^{13}$C glutamine (**A**). Incorporation of 1-$^{13}$C label ("+ 13C") into α ketoglutarate (**B**) and citrate (**C**) was measured after ~ 5 min, 12 and 24 hours. The 1-$^{13}$C label is not incorporated into succinate (**D**). Shown is mean ± S.D. for triplicate experiments. *$P$ < 0.05 (two-sided t-test), versus control cells. Control: cultured with 1 mM PAMO. Abundance of unlabeled ("all 12C") und $^{13}$C labeled metabolites was measured in cell extracts.

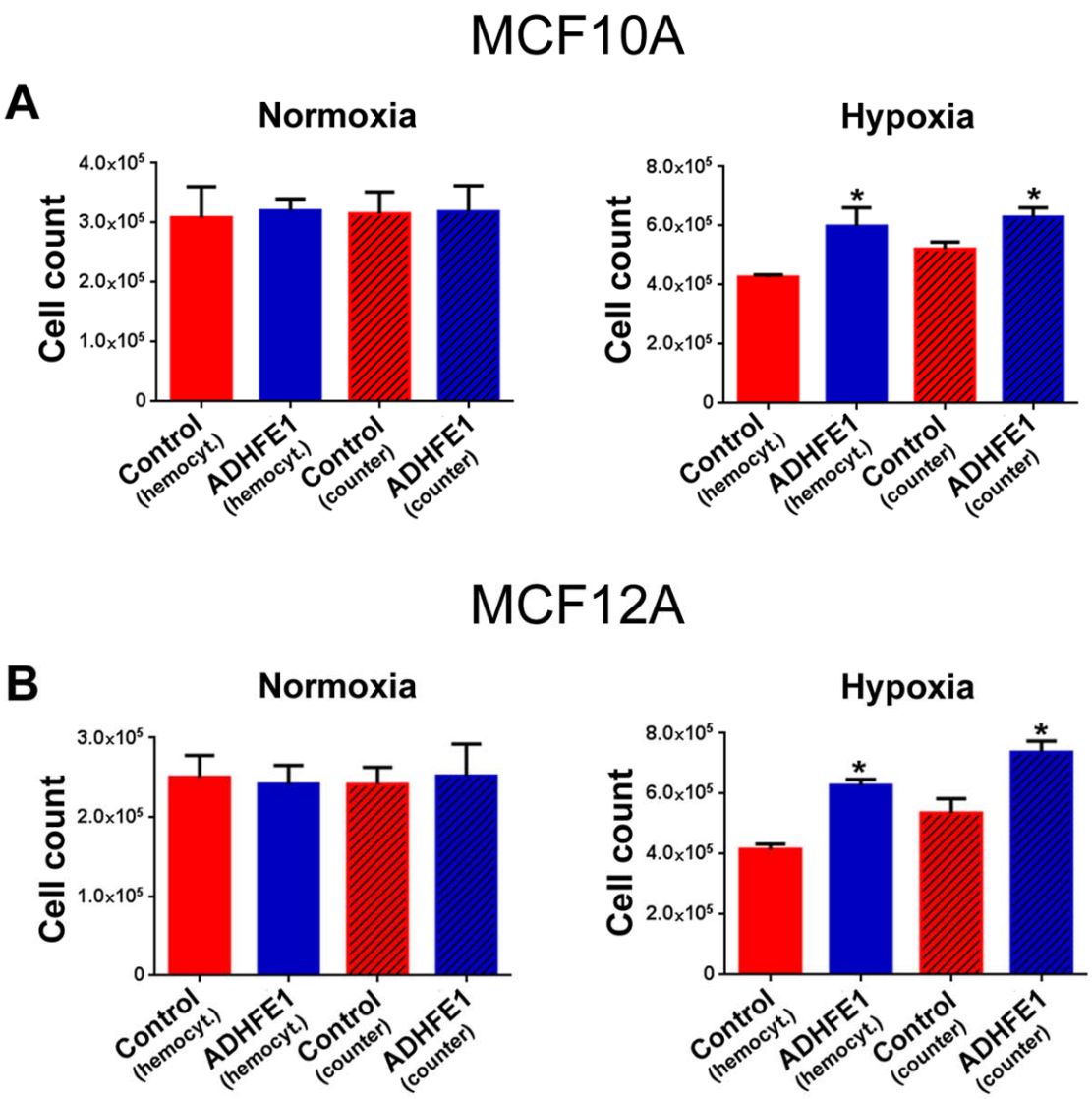


**Supplemental Figure 9. Increased proliferation of *ADHFE1*-overexpressing cells under hypoxia.** MCF10A (**A**) and MCF12A (**B**) cells were cultured under normoxic (21% oxygen) and hypoxic (0.5% oxygen) conditions for 2 days and cell numbers were determined by directly counting cells using both a hemocytometer ("hemocyt.") and an automated cell counter ("counter"). Cell counts of *ADHFE1*-overexpressing cells were significantly higher (30% to 50% increase) than those of vector control cells when cultured under hypoxia but there was no difference in cell numbers when these cells were cultured under normoxic conditions. Shown is mean ± S.D. for triplicate experiments. **P* < 0.05, versus vector control cells (two-sided t-test).

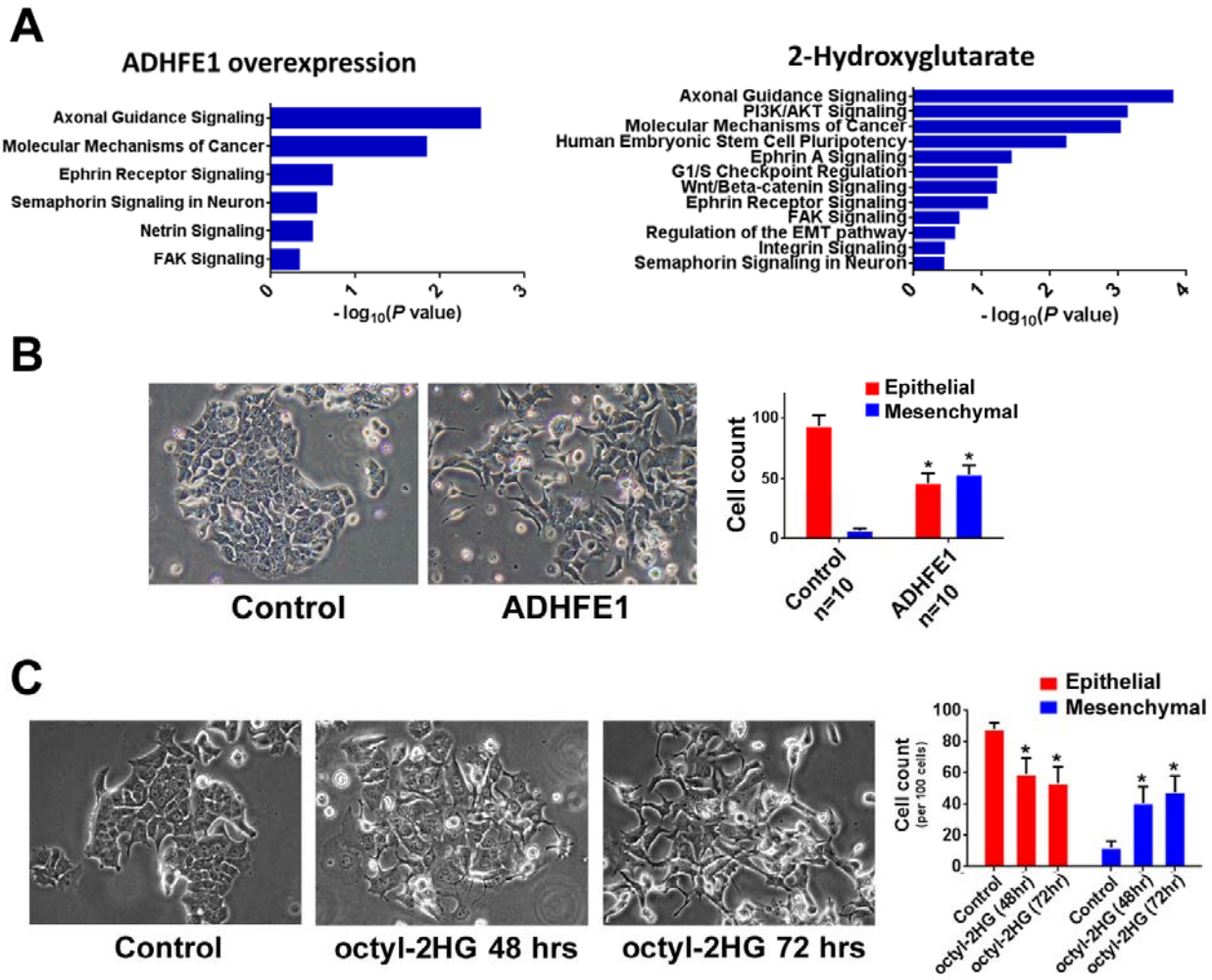


**Supplemental Figure 10. ADHFE1 and cell-permeable D-2-hydroxyglutarate (octyl-2HG) induce a mesenchymal phenotype in MCF7 breast cancer cells.** (**A**) Shown are Ingenuity pathways that are enriched for differently expressed genes comparing MCF7 cells with up-regulated ADHFE1 vs. vector control cells (left) and MCF7 cells treated with 1 mM octyl-2HG vs. cells treated with control compound, 1 mM PAMO (right). Analysis was performed with differentially expressed genes at a FDR < 5% and a fold change ≥ 1.5 cutoff. Enrichment *P* values are shown as $-\log_{10}$ ($P < 0.05$ and $P = 0.01$ correspond to 1.31 and 2 on the x-axis). Axon guidance signaling and molecular mechanisms in cancer are significantly enriched in both experimental settings. (**B**) *ADHFE1*-overexpressing MCF7 cells develop a mesenchymal phenotype as shown by a loss of cell-cell adhesion and a stellate-shaped morphology. Magnification: x200. Graph to the right shows quantitative analysis of cell morphology. Shown is mean ± S.D. for 10 counted areas (per 100 cells). *$P < 0.05$, versus control cells (two-sided t-test). (**C**) 1 mM octyl-2HG induces a mesenchymal phenotype in MCF7 cells. Control: 1 mM PAMO. *$P < 0.05$, versus control cells (two-sided t-test). Magnification: x200. Graph to the right shows quantitative analysis of cell morphology. Cell counts are shown as mean ± S.D. for 5 counted areas (per 100 cells).

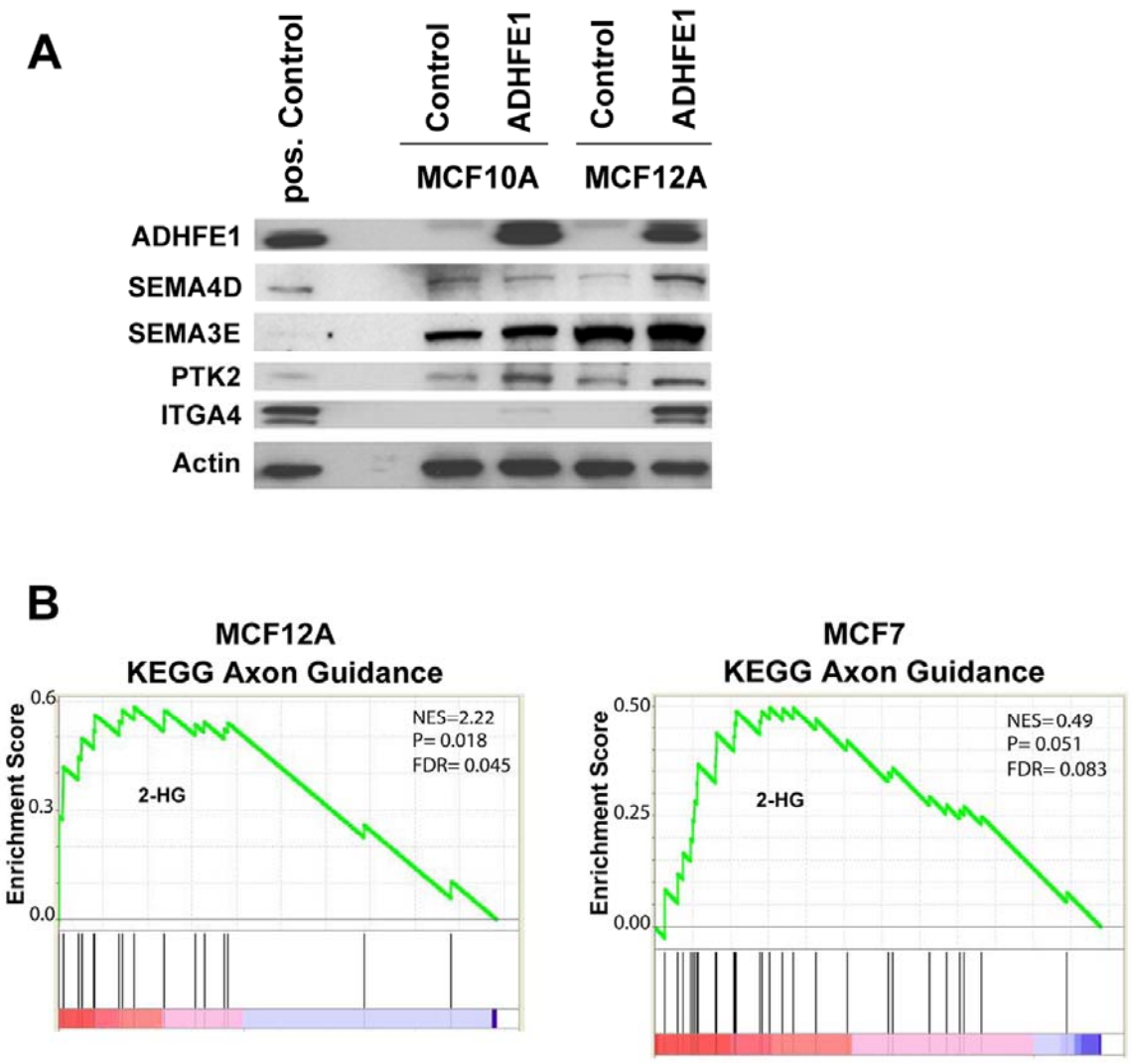


**Supplemental Figure 11. Induction of axon guidance signaling by both ADHFE1 and cell-permeable D-2-hydroxyglutarate (octyl-2HG**). (**A**) Western blot analysis of protein extracts from MCF10A and MCF12A cells constitutively overexpressing *ADHFE1*. The blot shows expression of proteins in the axon guidance pathway. (**B**) Gene set enrichment analysis based on KEGG pathways for MCF12A and MCF7 cells treated with octyl-2HG ("2HG"). Enrichment scores in the axon guidance pathway for differentially expressed genes comparing MCF12A and MCF7 cells treated with octyl-2HG for 48 hrs vs. control compound (1 mM PAMO)-treated cells. Graphs indicate enrichment for up-regulated genes (red colors) following octyl-2HG treatment.

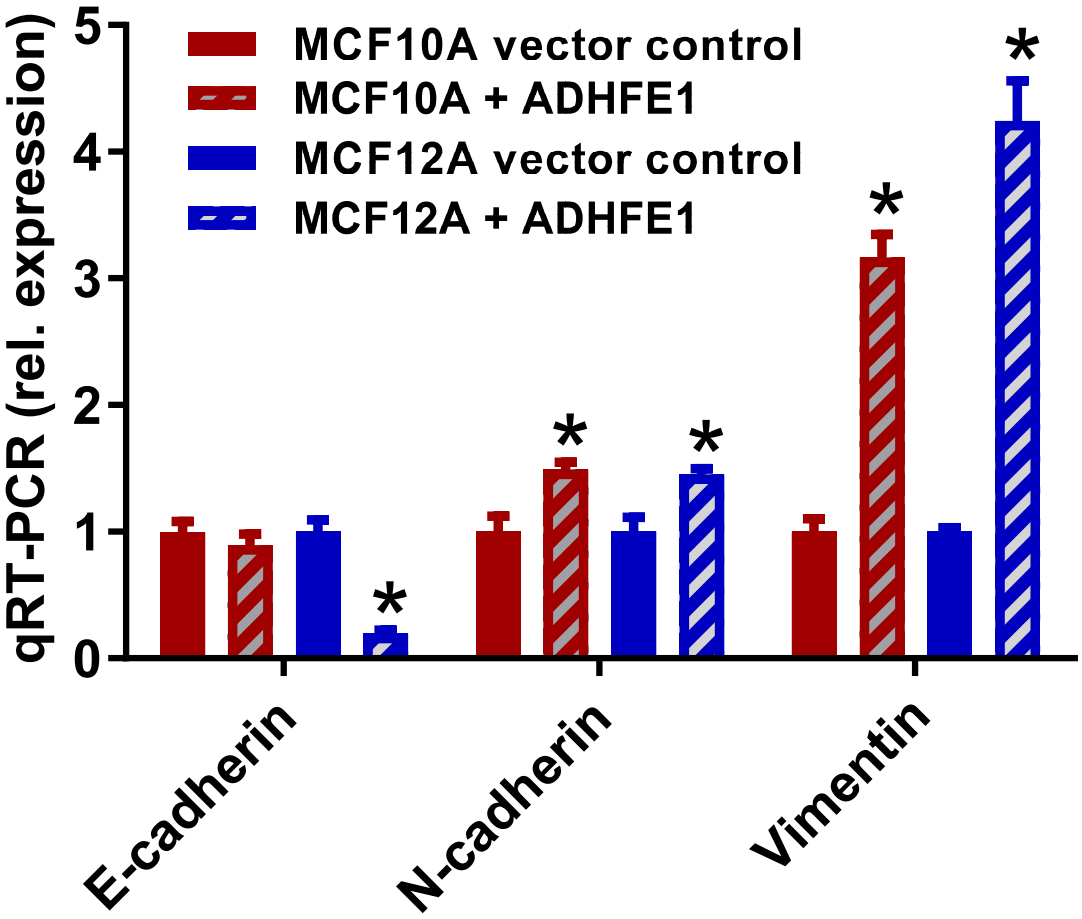


**Supplemental Figure 12. mRNA expression of epithelial to mesenchymal transition markers in breast epithelial cells with increased *ADHFE1*.** qRT-PCR analysis of E-cadherin (*CDH1*), N-cadherin (*CDH2*), and vimentin (*VIM*) expression in MCF10A and MCF12A cells with *ADHFE1* transgene vs. vector control cells. Shown is mean ± S.D. for triplicate measurements. **P* < 0.05, versus vector control cells (two-sided t-test). Expression in control cells was normalized to one as reference.

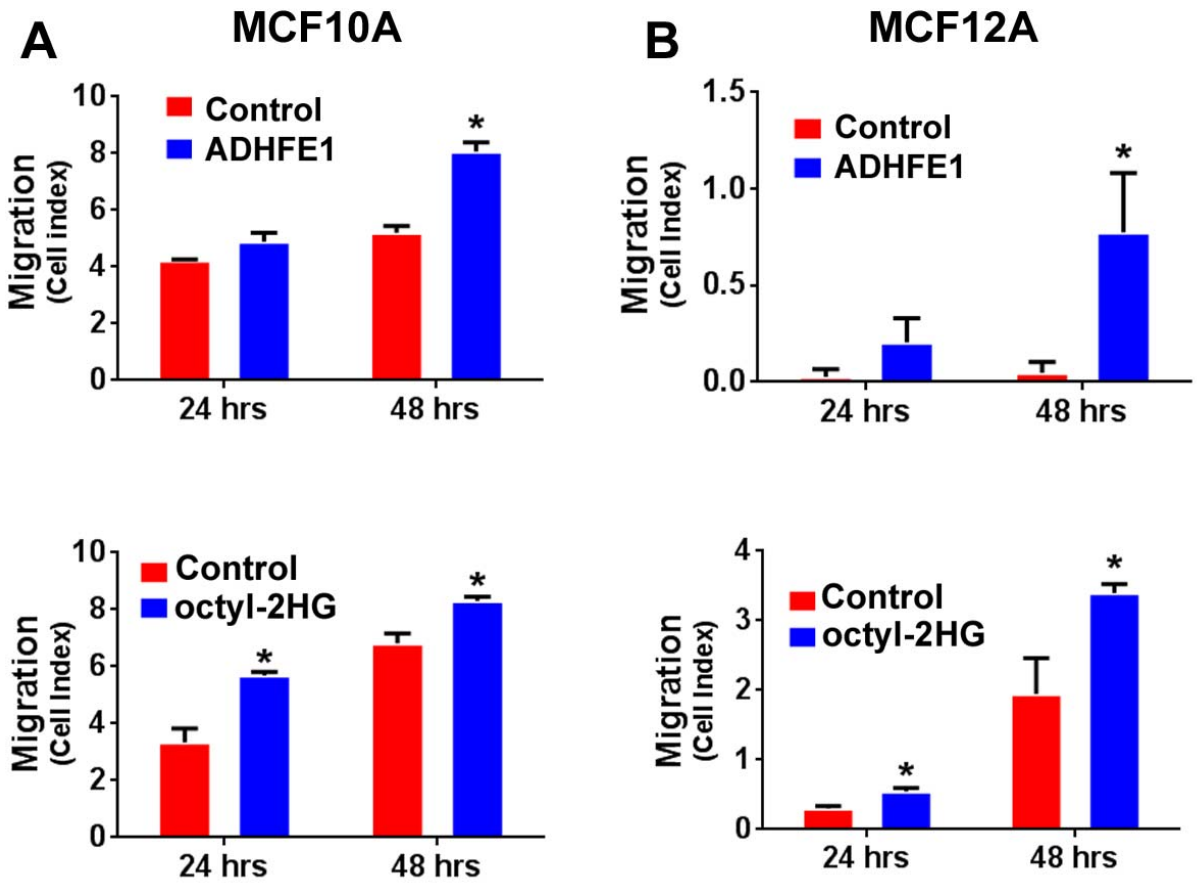


**Supplemental Figure 13. Up-regulated ADHFE1 and cell-permeable D-2-hydroxyglutarate augment migration of MCF10A and MCF12A cells.** Migration was examined using the xCelligence system, as described under Methods. $5x10^4$ cells were plated and migration of cells was monitored for 48 hours. (**A**) MCF10A cells and (**B**) MCF12A cells. The graphs show increased migration of *ADHFE1* transgene expressing cells vs. vector control cells (top) or cells treated with cell-permeable D-2-hydroxyglutarate (1 mM octyl-2HG) vs. control cells (bottom). Control cells received 1 mM PAMO. Shown is mean ± S.D. for triplicate experiments. *$P < 0.05$, versus control cells (two-sided t-test).

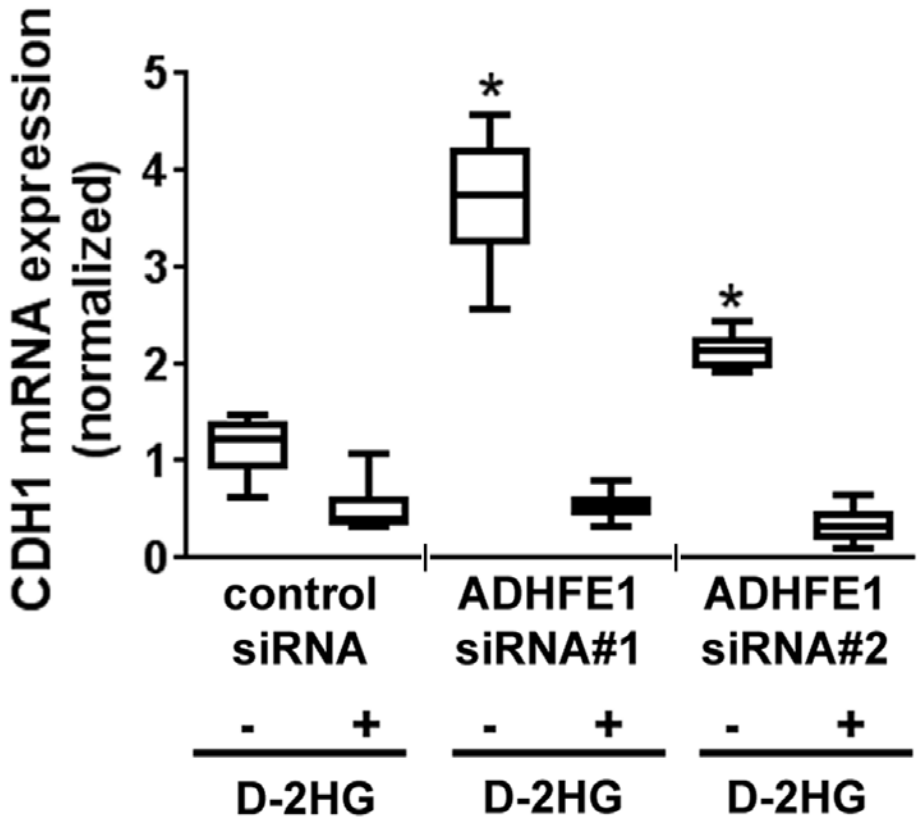


**Supplemental Figure 14. Cell-permeable D-2-hydroxyglutarate prevents the increase in epithelial characteristics following the down-regulation of *ADHFE1* with siRNA.** Treatment of MDA-MB-231 cells with *ADHFE1* siRNAs 1 & 2 increases the expression of the epithelial marker, *CDH1* (E-cadherin), in absence of exogenous 2HG. This increase is suppressed by cell-permeable D-2HG. * $P < 0.05$, versus control siRNA (two-sided t-test). Triplicate experiments. MDA-MB-231 cells were transfected with control siRNA, or siRNAs 1 & 2 targeting *ADHFE1*, in presence or absence of cell-permeable D-2HG, and *CDH1* mRNA expression was measured by qRT-PCR.

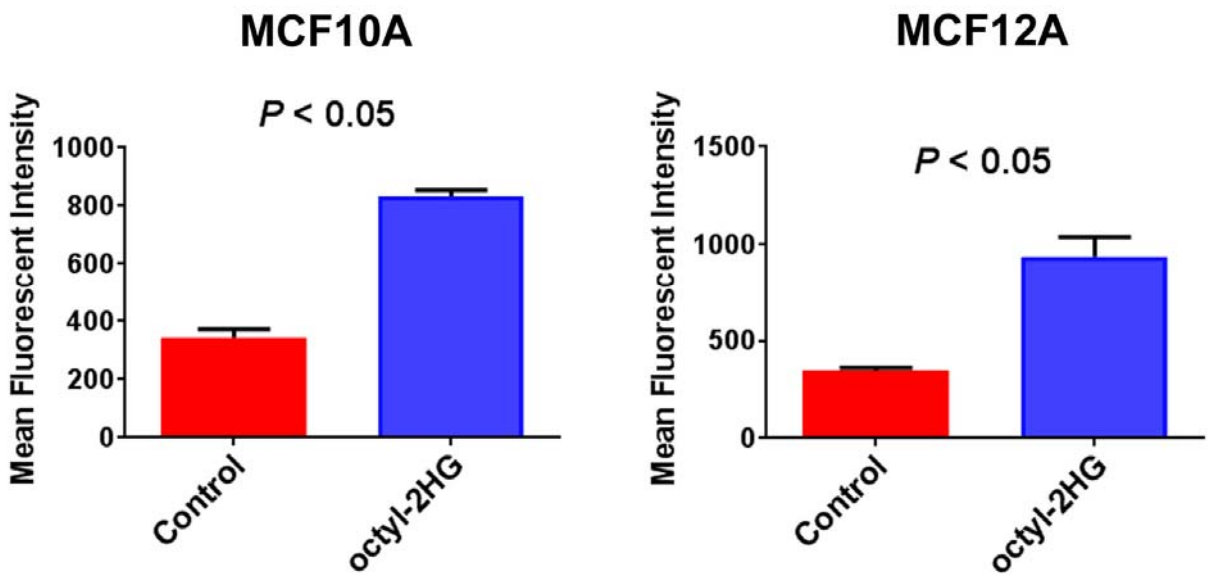


**Supplemental Figure 15. Increased superoxide in cells treated with cell permeable D-2HG.** The mitochondrial superoxide indicator, MitoSox, shows increased superoxide production in MCF10A and MCF12A cells treated with octyl-2HG. Cells were treated for 48 hrs with either 1 mM of octyl-2HG or the control compound, PAMO (Control), to determine if cell-permeable D-2HG induces mitochondrial ROS. Shown is mean ± S.D. for n = 4 experiments. Two-sided t-test for statistical significance testing.

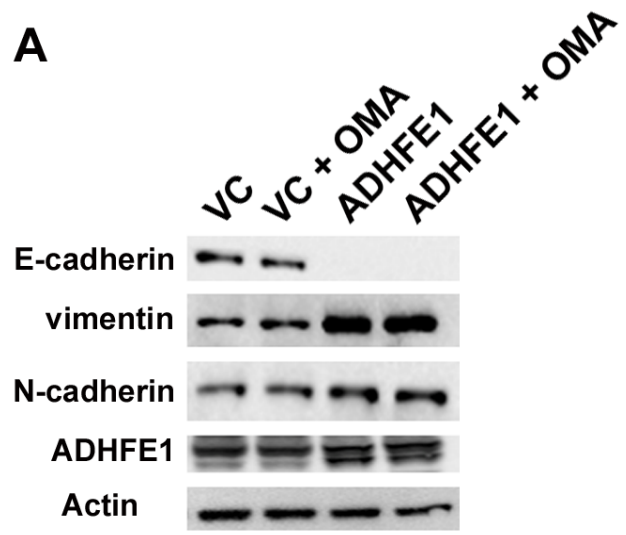


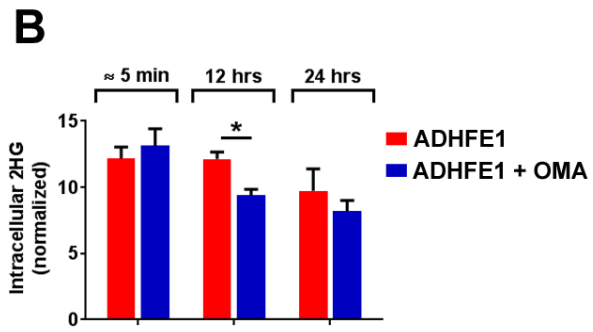


**Supplemental Figure 16. Expression of EMT markers in *ADHFE1*-overexpressing MCF12A cells treated with oxalomalate.** (**A**) Shown is a Western blot for EMT markers (epithelial marker, E-cadherin, and mesenchymal markers, vimentin and N-cadherin). Treatment of cells with oxalomalate (OMA), a competitive inhibitor of IDH1 & 2, did not alter expression of these markers. MCF12A cells +/- *ADHFE1* transgene were treated with 1 mM oxalomalate for 48 hrs when protein extracts were prepared. VC, vector control. (**B**) Effect of 1 mM oxalomalate on total 2HG levels in *ADHFE1*-overexpressing MCF12A cells. *$P < 0.05$, two-sided t-test. Shown is mean ± S.D. for triplicate experiments.

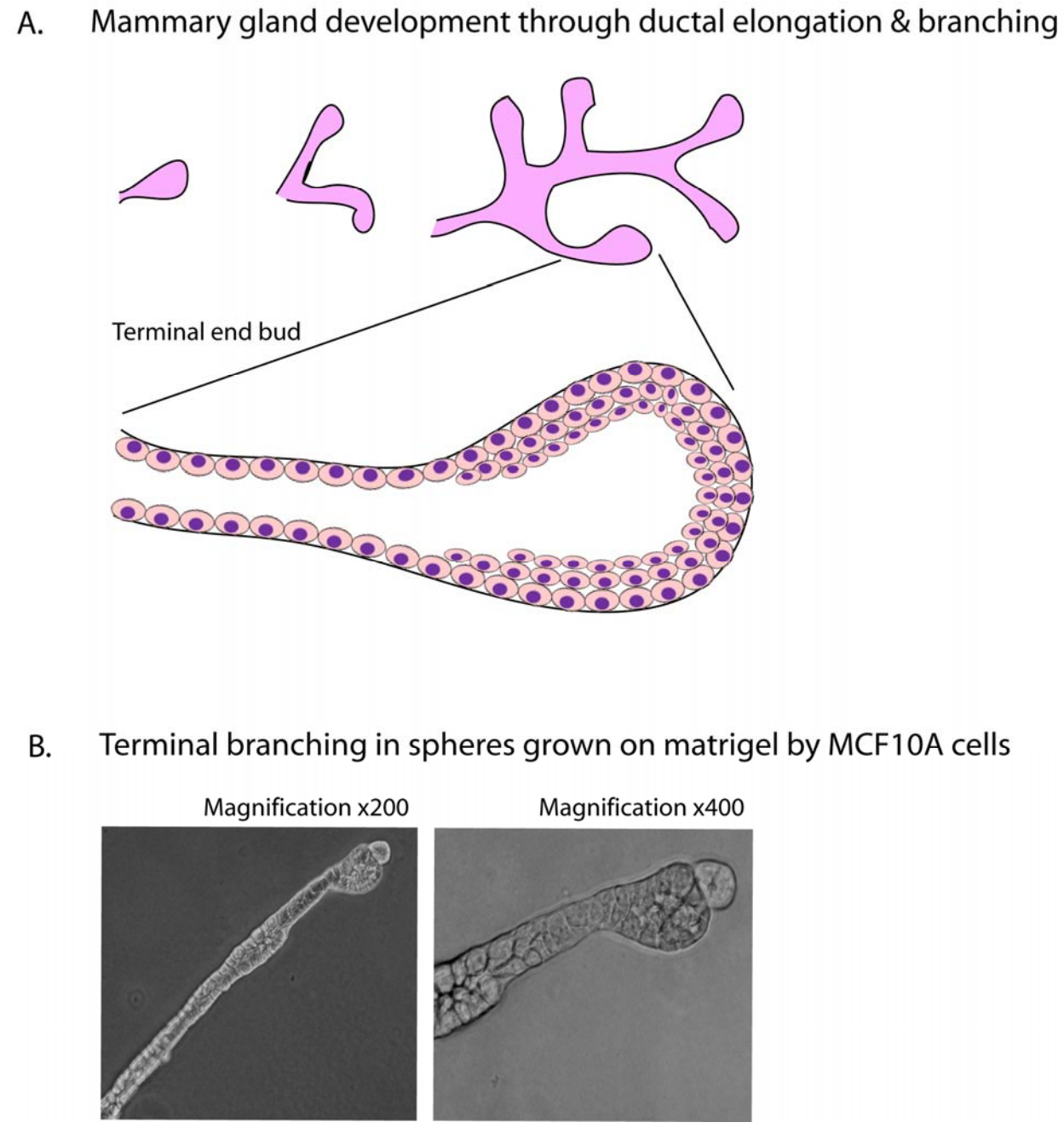


**Supplemental Figure 17. Duct-like structures that are formed by MCF10A cells in the sphere formation assay.** (**A**) Drawing showing mammary gland development. (**B**) Close up photographs of duct-like structures through terminal branching evolving from spheres formed by MCF10A cells.

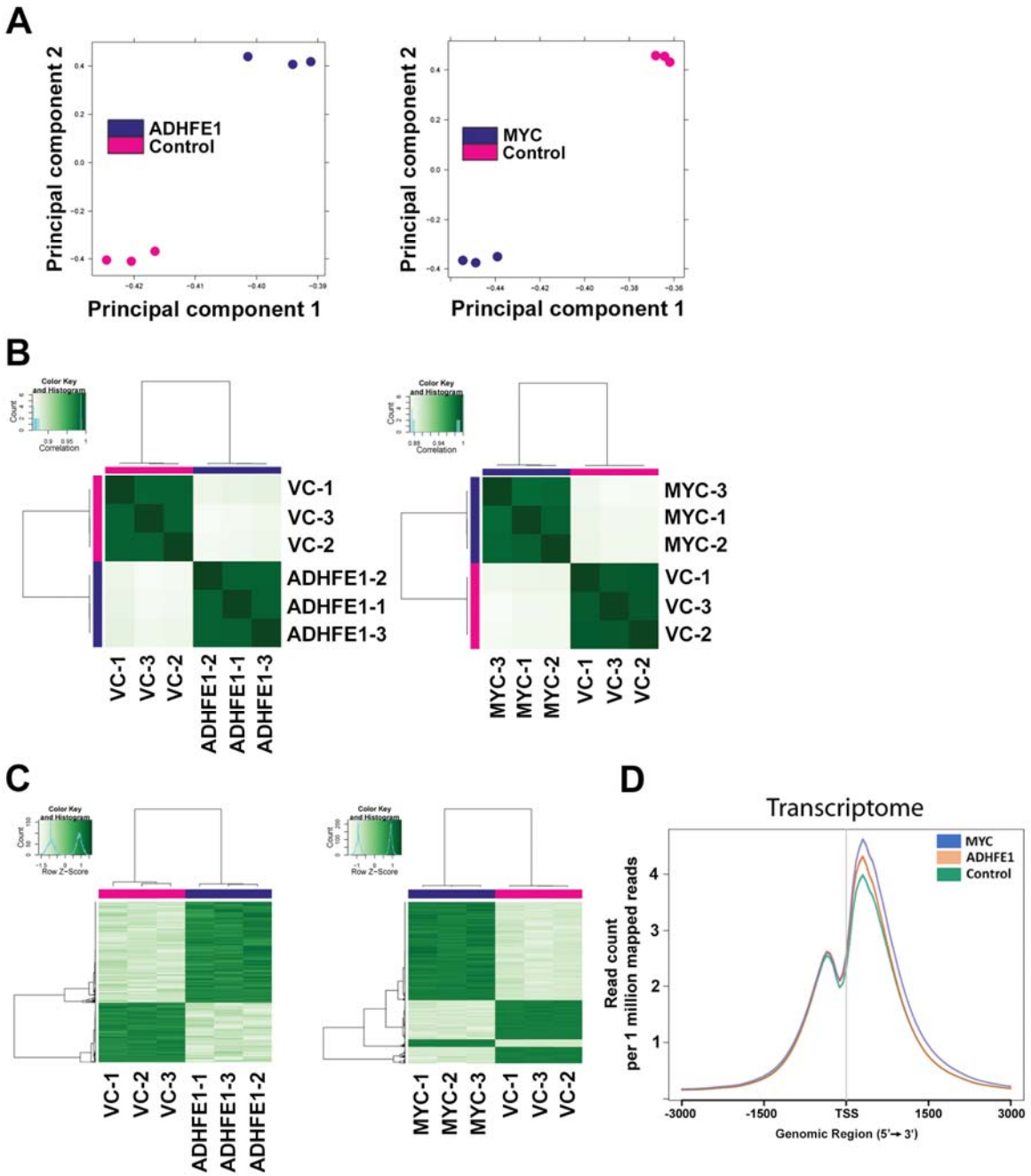


**Supplemental Figure 18. Chip-seq analysis of histone trimethylation at histone 3 lysine 4 (H3K4me3) in MCF7 cells.** (**A**) Principal component analysis plot shows a robust separation of vector control versus *ADHFE1*- or *Myc*-overexpressing MCF7 cells based on the consensus peaks for H3K4me3 in the chip-seq data. (**B**) A correlation heatmap for the same triplicate chip-seq experiments with vector control versus *ADHFE1*- or *Myc*-overexpressing MCF7 cells. (**C**) Heatmap showing H3K4me3 binding sites with a significant difference (FDR < 5%) between vector control and *ADHFE1*- or *Myc*-overexpressing MCF7 cells. Genomic loci with increased H3K4me3 (dark green) are more frequent in *ADHFE1*- or *Myc*-overexpressing than control cells. (**D**) H3K4me3 is transcriptome-wide increased in promoter regions of protein-coding genes in *Myc*- or *ADHFE1*-overexpressing MCF7 cells (FDR < 5%, vs. vector control cells).

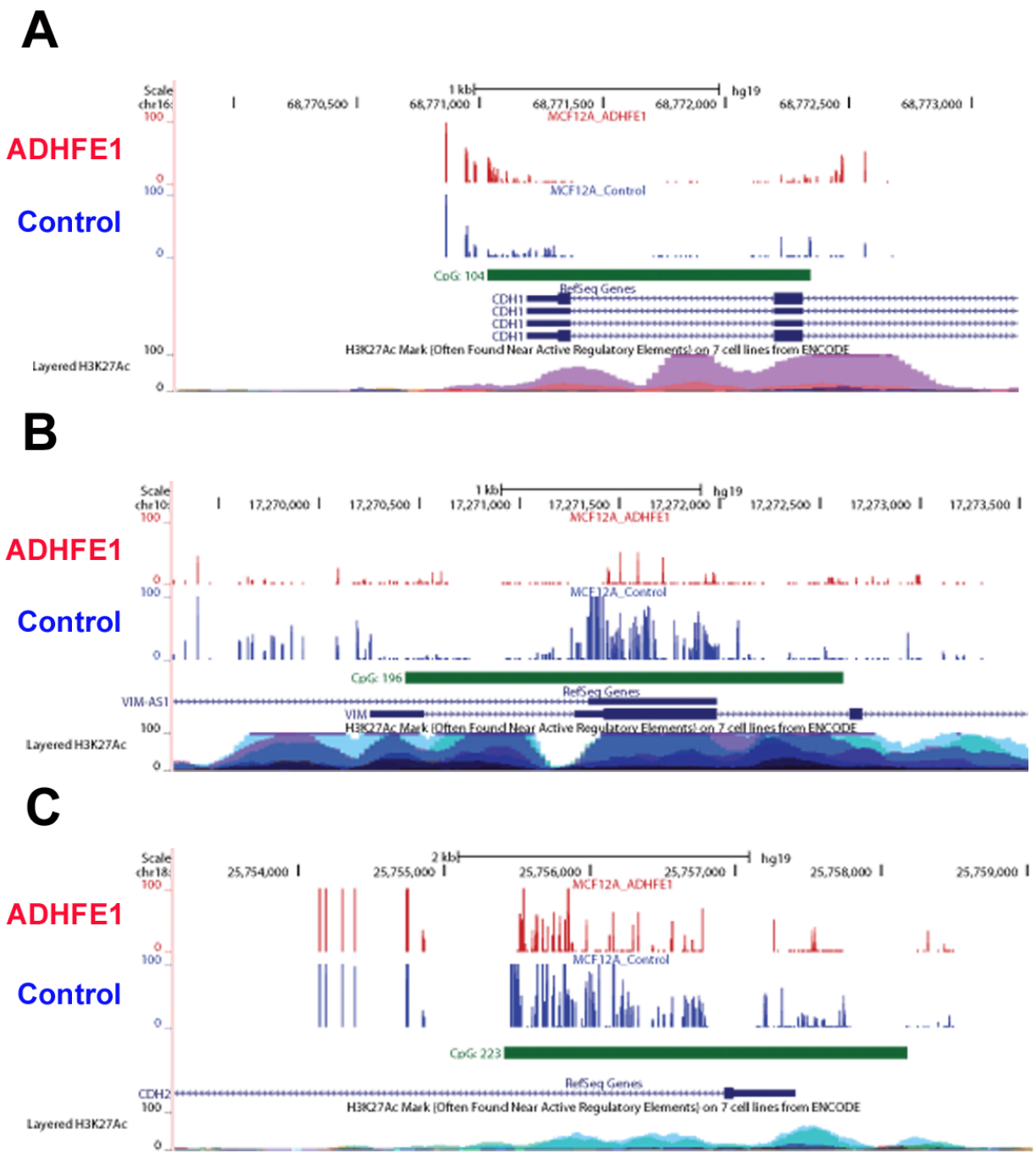


**Supplemental Figure 19. DNA methylation at CpG sites in three genomic loci encoding epithelial-to-mesenchymal transition markers comparing *ADHFE1*-overexpressing with vector control MCF12A cells.** DNA methylation analysis was performed using targeted bisulfide sequencing (see Methods). Shown are CpG methylation profiles near the transcription start site for the *CDH1* (E-cadherin) locus (**A**), *VIM* (vimentin) locus (**B**), and the *CDH2* (N-cadherin) locus (**C**). In the *ADHFE1*-overexpressing cells, CpG methylation increased at the *CDH1* locus and decreased at the *VIM* and *CDH2* loci. Red, CpG methylation in *ADHFE1*-overexpressing cells. Blue, CpG methylation in vector control cells. Scale: 0, no methylation at a CpG site; 100: complete methylation of a CpG site.

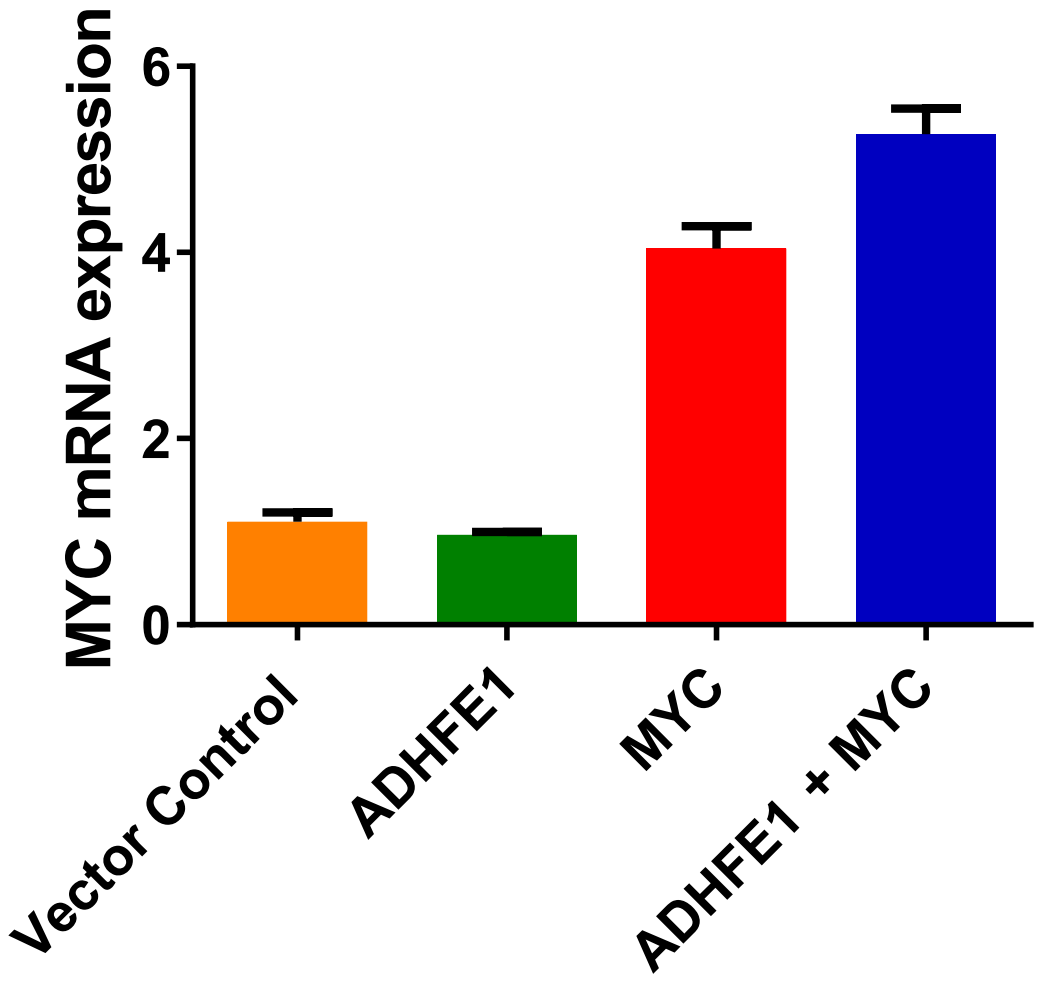


**Supplemental Figure 20. Upregulation of *MYC* mRNA after expression of a lentiviral *MYC* transgene in MCF7 cells.** To obtain stable cell lines overexpressing *MYC*, MCF7 cells -/+ *ADHFE1* transgene were infected with lentivirus containing the expression vector pCMV>Hs.MYC_IRES-eGFP and selected with neomycin (1600 µg/ml). Shown is mean ± S.D. for triplicate measurements.

## Supplemental Methods

**Reagents and lentiviral vectors.** Octyl-D-2HG ([2R]-2-hydroxyglutaric acid octyl ester), abbreviated as octyl-2HG in the text, and control compound [pentanedioic acid monooctylester (PAMO)] were custom synthesized by SLR Biosciences, Burlington, MA, and were added to cell culture medium in DMSO as solvent (1 µl per 2 ml culture medium). PAMO has cell permeability characteristics similar to 2HG and is also a control for octanol release. $^{13}$C-labeled L-Glutamine (1 $^{13}$C and 1-5 $^{13}$C, 99%) was purchased from Cambridge Laboratories, Inc. (Tewksbury, MA). N-acetylcysteine (NAC) and 3-Aminopyridine-2-carboxaldehyde thiosemicarbazone were obtained from Sigma (St. Louis, MO). Lentiviral constructs (pFUGW-CMV51p>Hs.ADHFE1-FLAG with C-terminal FLAG epitope tag and pFUGW-CMV51p control vector) were obtained from the Protein Expression Laboratory, Leidos Biomedical Research, Frederick National Laboratory for Cancer Research, MD. The FUGW lentiviral vector system has been described (1, 2). Subcloning for lentiviral reporter constructs was performed as follows: Gateway Multisite LR recombination was used to construct the final lentiviral reporter constructs from the Entry clones using the manufacturer's protocols (Life Technologies, Carlsbad, CA). pDest-663 was the Gateway Destination vector, which is a lentiviral vector containing a Gateway attR4-attR2 cassette based on a modified version of the pFUGW lentiviral vector and contains the enhanced polypurine tract and woodchuck regulatory element to provide higher titer virus. In addition, it contains an antibiotic resistance gene for puromycin resistance. Final expression clones were verified by restriction analysis and sequencing, and maxiprep DNA for lentivirus production was prepared using the GenElute XP purification kits (Sigma, St. Louis, MO).

**Orthotopic injection of MCF7 cells into the mammary fat pad of mice for tumor growth.** MCF7 cells were infected with lentiviral constructs to obtain constitutive expression of the target genes, *ADHFE1*, *MYC*, or both *ADHFE1* and *MYC*. To obtain stable cell lines overexpressing *MYC*, MCF7 cells -/+ *ADHFE1* transgene were infected with lentivirus containing the expression vector pCMV>Hs.MYC_IRES-eGFP and selected with neomycin (1600 µg/ml), which led to a 4- to 5-fold up-regulation of *MYC* in the selected cells (**Supplemental Figure 20**). Cells were inoculated into nonobese diabetic/severe combined immunodeficiency mice (NOD/SCID gamma, NOD.Cg-*Prkdc*$^{scid}$ *Il2rg*$^{tm1Wjl}$/SzJ, strain no. 005557, Jackson Laboratory, Bar Harbor, ME), as these mice do not require implantation of estrogen pellets for tumor growth of MCF7 cells. Five mice were housed per cage, and given autoclaved food and water ad libitum. Eight weeks old female mice were injected unilaterally with $5\times10^6$ cells in 100 µL of Matrigel/PBS (50:50) into the fourth abdominal fat pad by subcutaneous injection. Tumor growth was monitored weekly and measured externally using Vernier Calipers. Animals were sacrificed after 16 weeks when tumors in the *ADHFE1-MYC* grouped started to reach the critical size of 1500 $mm^3$. Tumor volume was calculated as $mm^3$ = [length × width$^2$]/2. The protocol for this experiment was reviewed and approved by the NCI *Animal Care* and Use *Committee* [Animal Study Protocol Number LHC-004-2] and experiments were performed in accordance with principles outlined in the *Guide for the Care and Use of Laboratory Animals at NIH.*

**2-Hydroxyglutarate and 4-hydroxybutyrate levels in tissue and cell lines.** Total 2-hydroxyglutarate (2HG) in cells was measured as previously described (3). The relative abundance of D- and L-2HG in breast tumors was measured using chemical derivatization of 2HG as recently described (4). Briefly, tumor tissue was homogenized with 10 volume of PBS. 50 µl

homogenate was mixed with 50 µl of internal standard (500 ng/ml of each L-and D-2HG-d3), followed by L-/D-2HG extraction with 500 µl of methanol. 200 µl of 20 mg/ml DATAN in a solution of dichloromethane and acetic acid was added to the dried down extracts, and the derivatization reaction was carried out for 20 min. After the reaction mixture was dried down, 200 µl of water was added for reconstitution, and 10 µl of sample was injected for L-/D-2HG analysis. The separation of L-/D-2HG derivatives was performed by a Waters Xterra MS C18, 125A 5 µm 2.1x150mm column, and a Waters Xevo TQ-S tandem mass spectrometer (MS) was used to monitor specific mass transitions of m/z363>147 (L/D-2HG) and 366>150 (L/D-2HG-d3, internal standard), respectively. The same protocol was used to measure D-2HG in cell pellets and culture medium.

4-Hydroxybutyrate was analyzed using gas chromatography (GC)-coupled MS (Agilent 7890A and Agilent 7000 QQQ) and a single reaction monitoring strategy with electron-impact ionization. For quantitation in tissue extracts, a serial dilution of 4-hydroxybutyrate was mixed with a fixed amount of [D27] myristic acid internal standard so that 0.02 to 500 pmol amounts of 4-hydroxybutyrate were injected into GC/MS. Tissue extracts were mixed similarly with the [D27] myristic acid internal standard, analyzed by GC/MS, and estimated for normalized 4-hydroxybutyrate levels using the standard curve. We calculated 4-hydroxybutyrate levels per mg frozen tissue weight.

**Metabolome analysis of cell lines.** We analyzed the absolute concentration of 116 metabolites in cell lines using the metabolome analysis package “Carcinoscope” provided by Human Metabolome Technologies (HMT) (Boston, MA). For metabolite measurements by HMT, cell extracts were obtained following the manufacturer’s protocol. Briefly, about 5 x $10^6$ cells were

washed twice with 5% mannitol wash buffer, and once with MilliQ water, followed by addition of 300 µl of methanol and 560 µl of Internal Standard solution and incubated at room temperature for 30 sec. The extracted solution was then transferred to microtubes and centrifuged (2,300 g) at 40°C for 5 min. The supernatant was transferred to filter units and further centrifuged at 9100 g and 40°C for approximately 3 hrs. The filtered extract was then lyophilized at 1000 Pa pressure in a vacuum evaporator at room temperature till all the liquid evaporated. Samples were stored at -80 until analyzed. Targeted quantitative analysis was performed by Human Metabolome Technologies, Inc. on 8 samples of cultured cells, MCF12A overexpressing ADHFE1 (n = 4) and vector control MCF12A cells (n=4) using capillary electrophoresis mass spectrometry (CE-MS) in the cation and anion analysis modes for analyzing cationic (n = 54) and anionic (n = 62) metabolites, respectively. These metabolites involved in glycolysis, pentose phosphate pathway, tricarboxylic acid cycle, urea cycle, and polyamine, creatine, purine, glutathione, nicotinamide, choline, and amino acid metabolisms were annotated according to the HMT metabolite database.

**Metabolic flux of $^{13}$C-labeled glutamine.** The incorporation of $^{13}$C glutamine into tricarboxylic acid (TCA) cycle intermediates was determined as previously described (5). To examine alterations in the metabolic flux of 1-$^{13}$C glutamine due to ADHFE1, MCF10A and MCF12A cells were grown in six-well plates in regular media until 80% confluent when medium was changed to RPMI medium containing 2 mM of [1-$^{13}$C] glutamine (Cambridge Laboratories) and 10% dialyzed FBS. Cells were washed with PBS and harvested after ~ 5 min, 12 hrs, and 24 hrs, counted, and were snap frozen using liquid nitrogen. To examine whether cell-permeable D-2HG induces reductive carboxylation of [1-$^{13}$C] glutamine, MCF10A and MCF12A cells were serum-

starved overnight and then exposed to either 1 mM octyl-2HG or control compound (PAMO) in RPMI medium containing 2 mM [1-$^{13}$C] glutamine. Cells were washed with PBS and harvested after ~ 5 min, 12 hrs, and 24 hrs, counted, and were snap frozen using liquid nitrogen. Subsequently, the obtained frozen cell pellets were transferred into 0.5 ml of 1:1 mixture of water:methanol, then sonicated for 1 min (30 sec pulse twice) and then mixed with 450 µl of ice cold chloroform. The resulting homogenate was then mixed with 150 µl of ice cold water and vortexed again for 2 min. The homogenate was incubated at -20°C for 20 min and centrifuged at 4°C for 10 min to partition the aqueous and organic layers. The aqueous and organic layers were combined and dried at 37°C for 45 min in an automatic Environmental Speed Vac system (Thermo Fisher Scientific). The extract was reconstituted in 0.5 ml of ice cold methanol: water (1:1) and filtered through 3 KDa molecular filter (Amicon Ultracel-3 membrane, Millipore Corporation, Hayward, CA) at 4° C for 90 min to remove proteins. The filtrate was dried at 37°C for 45 min using the Speed Vac and stored at -80°C until mass spectrometry (MS) analysis. Prior to MS analysis, the dried extract was resuspended in 50 µl of methanol:water (1:1) containing 0.1% formic acid and delivered to the MS via normal phase chromatography using a Luna Amino column (4um, 100A 2.1x150mm, Phenominex). Ten microliters of extract were injected and analyzed using a 6490 QQQ triple quadrupole mass spectrometer (Agilent Technologies, Santa Clara, CA) coupled to a 1290 series HPLC system via Selected Reaction Monitoring. Metabolites were targeted in both positive and negative ion mode, ESI voltage was +4000 V in positive ion mode and –3500 V in negative ion mode. Approximately 9–12 data points were acquired per detected metabolite. Mass isotopomer distributions were calculated using the formula [fractional incorporation = $^{13}$C/$^{13}$C + $^{12}$C) x100] and corrected for natural abundance.

**Chromatin immunoprecipitation coupled with high-throughput sequencing (ChIP-Seq) analysis of histone trimethylation at histone 3 lysine 4 (H3K4me3).** To examine genome-wide histone modification in *ADHFE1*- and *MYC*-overexpressing cells, we cultured MCF7 control cells and cells overexpressing these genes in triplicates and crosslinked DNA and protein directly in the culture medium with 1% formaldehyde solution for 10 min at room temperature. Chromatin was then fragmented to 150-200 bp by 15 cycles of sonication (30s on/30s off) (Diagenode Bioruptor, Liege, Belgium). Fragmented chromatin from $2\times10^7$ cells and 5 μg of antibody against H3K4me3 (Abcam, ab8580) was used to perform the ChIP experiments using the High Sensitivity ChIP-IT Kit (Active Motif, Carlsbad, CA). Subsequently, ChIP-seq libraries were prepared using the Illumina TruSeq ChIP Sample Prep Kit with compatible indexed adaptors according to the manufacturer's instruction. Equal amounts of libraries were pooled for cluster generation and sequenced with an Illumina NextSeq500 system with 2 × 75 bp paired-end reads. On average, we generated 76 million PE reads per sample, and at least 85% of the reads were uniquely mapped to the human genome version hg19 using Bowtie2. Alignment was further cleaned by removing duplicated reads or reads mapped to the blacklist regions downloaded from UCSC table browser (http://hgwdev.cse.ucsc.edu/cgi-bin/hgFileUi?db=hg19&g=wgEncodeMapability). Peak calling was performed using MACS2, and the fraction of reads in peaks (FRiP) was at least 0.39 for H3K4me3. The quality of the peaks was also accessed using the Irreproducible Discovery Rate (IDR) framework with a 1% threshold. A differential binding analysis of ChIP-Seq peak data was performed with the *DiffBind* package. We generated a consensus peakset for each sample and utilized *DESeq2* for the differential binding analysis to calculated fold difference and *P* value for each binding site.

Peaks were annotated by the *ChIPpeakAnno* package, and assigned to the nearest gene TSS. ChIP-seq peaks were visualized by either IGVTools or ngs.plot to create density plot based on the read count per million mapped reads (RPM).

**DNA methylation analysis using bisulfide sequencing.** To examine DNA methylation patterns in ADHFE1-overexpressing cells, MCF12A vector control and ADHFE1-overexpressing cells were cultured and genomic DNA was extracted using the Qiagen DNA isolation kit (Qiagen, Valencia, CA). Bisulfide DNA libraries were constructed using the Accel-NGS Methyl-Seq DNA Library Kit from Swift Biosciences (Ann Arbor, MI). Libraries were captured with The SeqCap Epi CpGiant Enrichment Kits from Roche NimbleGen (Madison, WI), which covers more than 5.5 million CpG sites. Samples were multiplexed and sequenced on the Illumina Nextseq500 system with the 75 bp paired end mode. Raw reads were aligned to hg19 using Bismark with 5' and 3' trimming and deduplication. At least 75% reads were deduplicated and uniquely aligned. Analysis of differential methylation was conducted in R using the methylKit package with either single base pair or 200-bp titling of the target capture set.

**Hypoxia treatment and D-2HG measurements.** $1x10^6$ cells per well were seeded in a 100 mm petri dishes (n=3) with regular culture media and incubated in standard $CO_2$ incubator with 21% oxygen, overnight. For hypoxia treatment, the cells were transferred into a hypoxia chamber supplied with 0.5% oxygen, 5% carbon dioxide and 94.5% nitrogen, and maintained at $37^0$C and standard humidity. To measure intracellular and secreted D-2HG, cells were kept under hypoxia for 24 hrs while the aerobically cultured cells were maintained in the standard incubator. After completion of 24 hrs in hypoxia or normoxia, cell medium was collected. Subsequently, the cells

were trysinized, washed with PBS, counted, and equal number of cells ($1x10^6$) from each treatment were pelleted for measurement of D-2HG. To determine growth rates of cells under either hypoxia or normoxia, cells were incubated overnight under aerobic condition and then cultured under either 0.5% or 21% oxygen for 48 hrs before cell numbers were counted with a hemocytometer or the TC10 Automated Cell Counter (Bio-Rad, Hercules, CA).

**Migration and invasion assay.** Migration and invasion were examined using the xCelligence System technology (Roche Applied Science/ACEA Biosciences, Inc, San Diego, CA) for real-time monitoring of cellular processes with electronic cell sensor arrays, according to the manufacturer's instructions. Briefly, cells were plated onto CIM-Plate 16 and the migratory and invasive capacity of cells was determined using the xCelligence system (Roche Diagnostics, Indianapolis, IN). For the invasion assay, the membrane in the top chamber of the CIM plate was coated with 30 µl of a 1:20 dilution of Matrigel (BD Biosciences, San Jose, CA) while this chamber remained uncoated for the migration assay. 100 µl of serum free media containing 50,000 cells was added to the upper chamber for plating (in triplicates, wells coated with Matrigel for the invasion assay or without Matrigel for the migration assay) and the lower chamber was filled with 10% FBS cell culture media. For 2HG treatment, serum-free media containing either 1 mM octyl-2HG or 1 mM control compound was added to the upper chamber. Loaded CIM-Plates were placed into the xCelligence analyzer and electrical impedance was measured every 15 minutes over a 48 hrs period. 1 mM octyl-2HG increased intracellular D-2HG concentrations by about 100-fold in a 48 hrs exposure experiment (3). The invasion index was calculated from the cell index ratio for Matrigel-coated wells and uncoated wells (the Cell index was determined per manufacturer's instructions).

**Iron measurements in mitochondria.** HMEC-MYC were cultured in 150 mm dishes (n = 4) in mammary epithelial growth medium (MEGM; Lonza, Allendale, NJ), and *MYC* was induced with 300 nM tamoxifen. After 96 hrs, cells were washed twice with PBS, harvested, counted, and mitochondria were isolated with the Mitochondria Isolation Kit (Thermo Fisher Scientific, # 89874) from $2x10^7$ cells according to the manufacturer's protocol. Iron was measured by inductively coupled plasma-mass spectrometry (ICP-MS) using a NexION 350D (Perkin Elmer, Shelton, CT) under DRC mode. Mitochondria was digested with 100 µl trace metal nitric acid (Fisher Chemical, Fairlawn, NJ) for 15 min a 65˚C water bath. Samples were allowed to cool and 100 µl of hydrogen peroxide (Optima grade, Fisher Chemical) was added and the digestion repeated. Samples were resuspended to a final volume of 500 µl with 2% nitric acid. Standard curves were generated using certified ICP-MS grade standards for quantitative analysis (SPEX CertiPrep, Metuchen, NJ). The iron 54 isotope was measured using ammonia gas at a flow rate of 0.6 ml/min and a 0.75 RPQ. Sulfur was measured by mass shifting to the SO48 isotope using DRC mode with oxygen gas at a 1.2 ml/min flow rate and a 0.5 RPQ. Gallium and beryllium were used as internal standards for iron and sulfur, respectively. Iron values were normalized to sulfur values for each sample.

**References**


1. Lois C, Hong EJ, Pease S, Brown EJ, and Baltimore D. Germline transmission and tissue-specific expression of transgenes delivered by lentiviral vectors. *Science.* 2002;295(5556):868-72.

2. Campeau E, Ruhl VE, Rodier F, Smith CL, Rahmberg BL, Fuss JO, Campisi J, Yaswen P, Cooper PK, and Kaufman PD. A versatile viral system for expression and depletion of proteins in mammalian cells. *PLoS One.* 2009;4(8):e6529.

3. Terunuma A, Putluri N, Mishra P, Mathe EA, Dorsey TH, Yi M, Wallace TA, Issaq HJ, Zhou M, Killian JK, et al. MYC-driven accumulation of 2-hydroxyglutarate is associated with breast cancer prognosis. *J Clin Invest.* 2014;124(1):398-412.

4. Struys EA, Jansen EE, Verhoeven NM, and Jakobs C. Measurement of urinary D- and L-2-hydroxyglutarate enantiomers by stable-isotope-dilution liquid chromatography-tandem mass spectrometry after derivatization with diacetyl-L-tartaric anhydride. *Clin Chem.* 2004;50(8):1391-5.

5. Dasgupta S, Putluri N, Long W, Zhang B, Wang J, Kaushik AK, Arnold JM, Bhowmik SK, Stashi E, Brennan CA, et al. Coactivator SRC-2-dependent metabolic reprogramming mediates prostate cancer survival and metastasis. *J Clin Invest.* 2015;125(3):1174-88.